

Supporting Information

The Impact of “Empty-Corner” Tetrahedra in the Synthesis of MFI Zeolite type: Unveiling Selenium Stereoactivity

Mishel Markovski^a, Abdallah Amedlous^a, Eddy Dib^{a,b}, Anna Kaleta^{a,c}, Francesco Dalena^a, Davide Salusso^d, Mathias Barreau^a, Diogenes Honorato Piva^a, Marco Giuseppe Geloso^a, Aymeric Magisson^a and Svetlana Mintova^{a*}

^a Université de Caen Normandie, ENSICAEN, CNRS, LCS, Laboratoire Catalyse et Spectrochimie, 14000 Caen, France

^b CEMHTI, CNRS, University of Orléans, 1D avenue de la Recherche Scientifique, 45071, Orléans, France

^c Institute of Physics, Polish Academy of Sciences, PL-02-668 Warsaw, Poland

^d European Synchrotron Radiation Facility, CS 40220, 38043 Grenoble Cedex 9, France

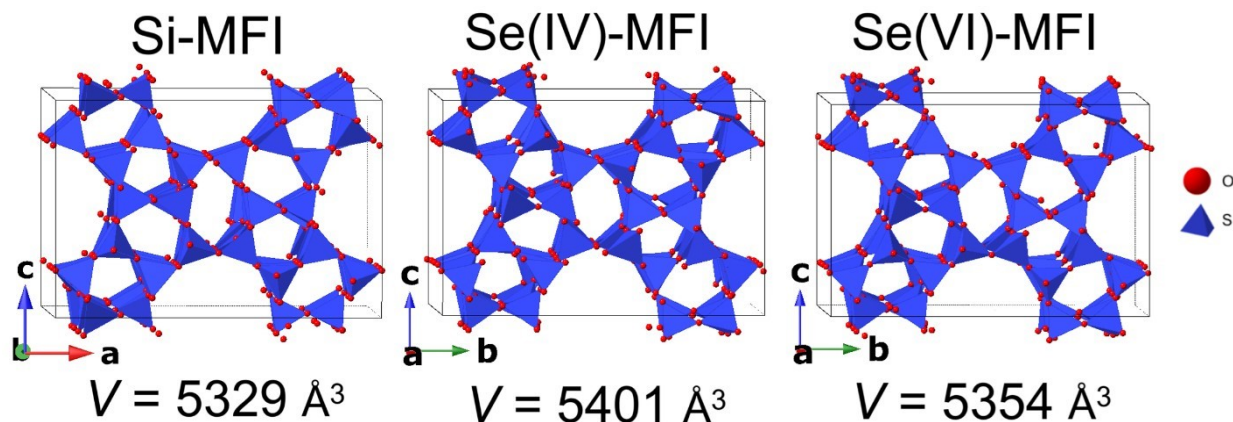


Figure S1. Semantical models of the unit cells from e Database of Zeolite Structures⁵: **a)** Si-MFI demonstrating an orthorhombic structure, **b)** Se(IV)-MFI and **c)** Se(VI)-MFI, both revealing monoclinic structures, with indication of Le Bail calculated unite cell volumes.

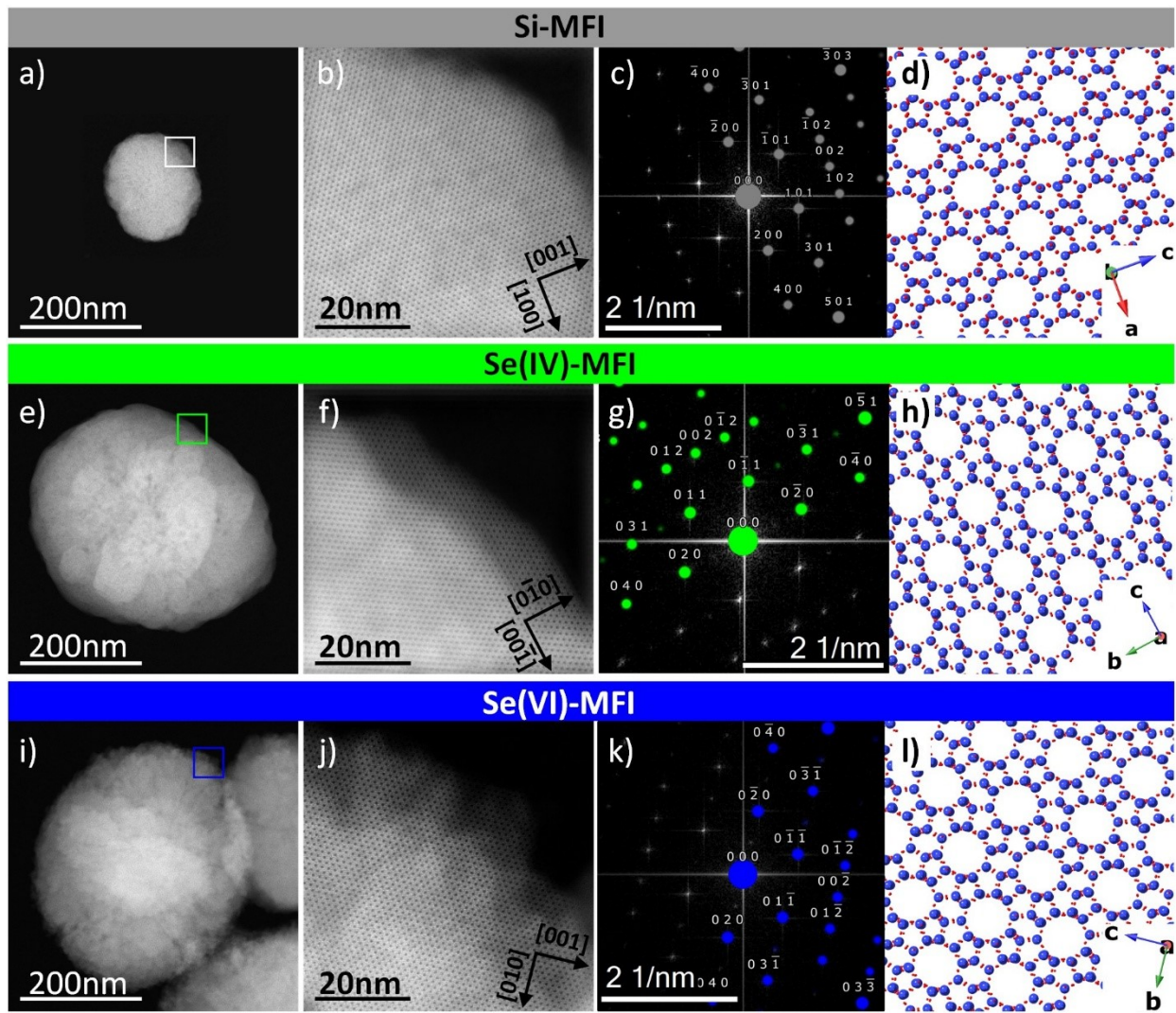


Figure S2. STEM images of isolated particles: Si-MFI (a), Se(IV)-MFI (e) and Se(VI)-MFI (i). Panels b, f, and j show high-resolution (HR) magnifications of the areas outlined by squares in panels a, e, and h, respectively, revealing their crystalline structure. Fast Fourier Transforms (FFTs) derived from the HR images in panels b, f, and j are shown in panels c, g, and k. Crystal structure models, based on XRD data (Figure S1 and Table 1), rotated to match the crystal orientation of the analyzed particles (i.e. [010] zone axis for Si-MFI, and [100] zone axis for both Se(IV)-MFI and Se(VI)-MFI) are depicted in panels d, h, and l. The FFT diffraction patterns calculated from these models (panels d, h, l) are superimposed with colored-coded reflexes and labeled hkl-indices. Crystallographic directions determined through FFT matching procedure are indicated by black arrows in panels b, f, j.

Table S1. Textural properties of Si-MFI, Se(IV)-MFI, and Se(VI)-MFI zeolite samples.

Sample	Surface area S_{BET} (m^2/g)	Micropore surface area S_{micro} (m^2/g)	Total Pore volume (cm^3/g)	Micro Pore volume (cm^3/g)
Si-MFI	534	314	0.31	0.16
Se(IV)-MFI	464	240	0.29	0.12
Se(VI)-MFI	472	240	0.29	0.12

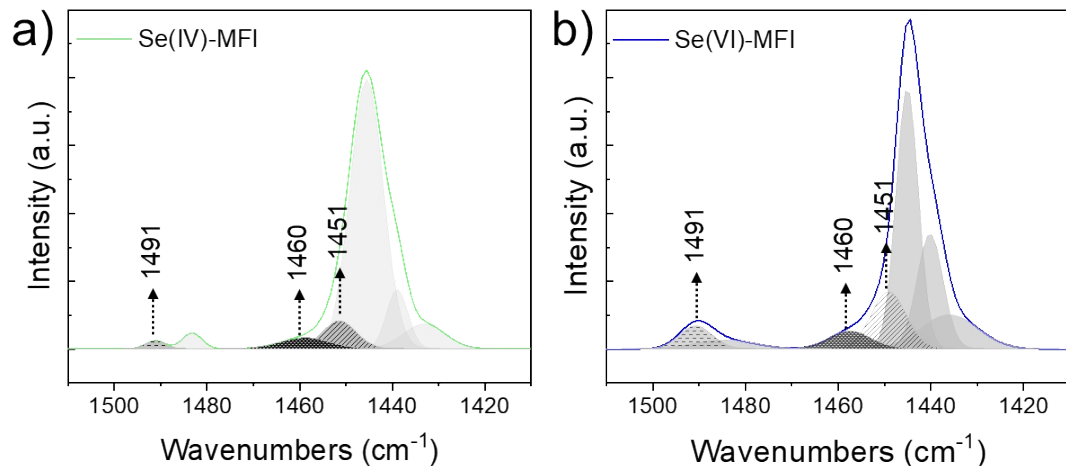


Figure S3. Deconvolution of the FT-IR spectra in the region 1550–1400 cm^{-1} of samples Se(IV)-MFI (a) and Se(VI)-MFI (b) after Py adsorption at 25 °C (2.022 torr).

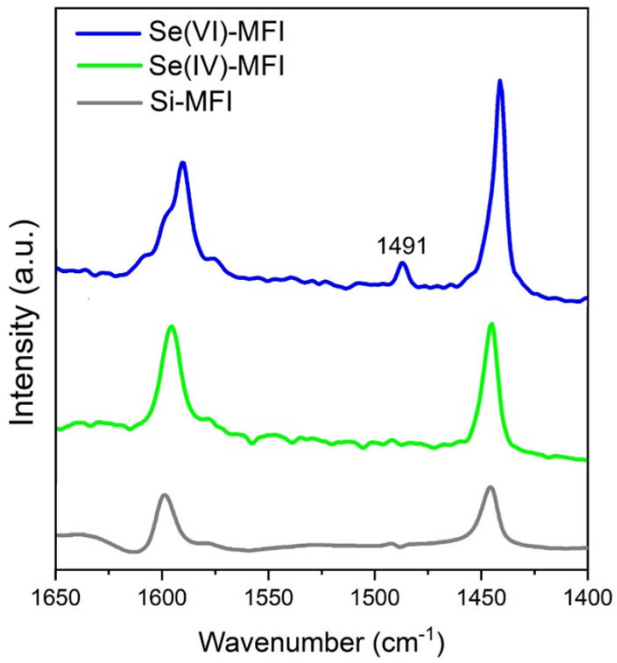


Figure S4. FT-IR spectra of samples Si-MFI, Se(IV)-MFI and Se(VI)-MFI after desorption of pyridine at 50 °C. All the spectra were obtained by subtraction the spectrum after activation and normalized to sample mass.

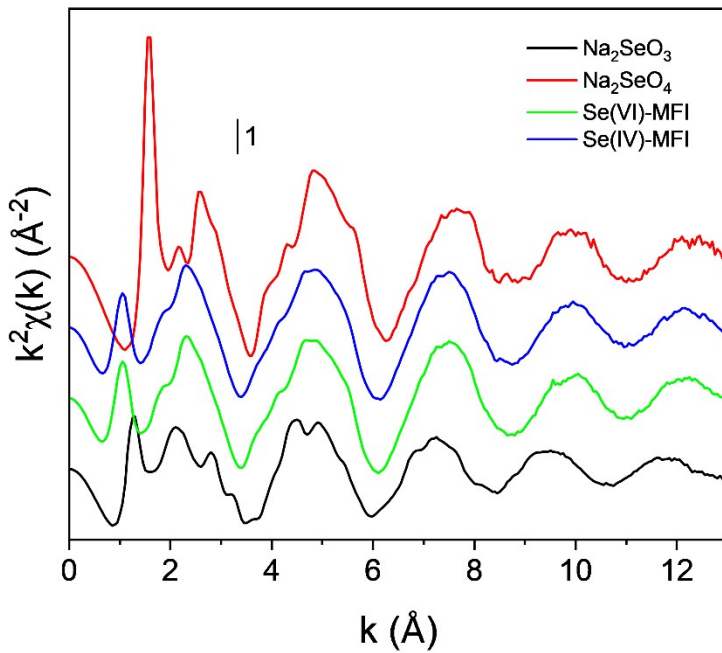


Figure S5. Stacked ex-situ k^2 -weighted EXAFS spectra of Se(IV)-MFI and Se(VI)-MFI samples compared with references Na_2SeO_3 and Na_2SeO_4 .

References

1. Y. Jia, J. Wang, K. Zhang, W. Feng, S. Liu, C. Ding and P. Liu, *Microporous Mesoporous Mater.*, 2017, 247, 103–115.
<https://doi.org/10.1016/j.micromeso.2017.03.035>
2. O. Mathon, A. Beteva, J. Borrel, D. Bugnazet, S. Gatla, R. Hino, I. Kantor, T. Mairs, M. Munoz, S. Pasternak, F. Perrin and S. Pascarelli, *J. Synchrotron Radiat.*, 2015, 22, 1548–1554.
<https://doi.org/10.1107/S1600577515017786>
3. M. Barreau, M. G. Geloso, D. Salusso, T. Spanjersberg and R. Zhang, *European Synchrotron Radiation Facility Dataset*, 2027.
<https://doi.org/10.15151/ESRF-ES-1992582793>
4. B. Ravel and M. Newville, *J. Synchrotron Radiat.*, 2005, 537–541.
<https://doi.org/10.1107/S0909049505012719>.
5. Database of Zeolite Structures approved by the Structure Commission of the International Zeolite Association (IZA-SC) <https://www.iza-structure.org/databases/>